Helicopter Roll-Axis Instabilities induced by Pilot Cyclic Control: A Physical Explanation

Marilena D. PAVEL*,[1], Achim IONITA[2]

*Corresponding author
*,[1]Delft University of Technology, Faculty of Aerospace Engineering,
Kluyverweg 1, 2629HS Delft, The Netherlands,
m.d.pavel@tudelft.nl
[2]INCAS – National Institute for Aerospace Research "ElieCarafoli",
B-dul Iuliu Maniu 220, Bucharest 061126, Romania
ionita.achim@incas.ro

DOI: 10.13111/2066-8201.2018.10.3.12

Received: 16 January 2018/ Accepted: 14 June 2018/ Published: September 2018

Aerospace Europe CEAS 2017 Conference,
16th-20th October 2017, Palace of the Parliament, Bucharest, Romania
Technical session & Workshop Rotorcraft

Abstract*: The main objective of this paper is to give a basic understanding of the mechanisms through which pilot cyclic inputs in lateral cyclic interacts with high-order rotor dynamics destabilizing the helicopter roll motion. The paper will use a "Newtonian formulation" representing the main forces acting on the airframe body-rotor system as the pilot applies his/her control. It will be demonstrated that pilot lateral controls applied through his/her arm (which may involve also pilot biodynamics, i.e. the dynamics of pilot neuromuscular inputs and contraction dynamics of his/her muscles) may excite much higher-order frequency rotor dynamics than thought at the present.*

Key Words*: Helicopter, Pilot Assisted Oscillations, Rotorcraft Pilot Couplings, Lead-lag mode, Rotor dynamics*

1. INTRODUCTION

The peculiarity of rotorcraft w.r.t. fixed-wing aircraft is that low-frequency pilot inputs can generate high-frequency blade excitations. This is because of the fact that, in contrast with fixed-wing aircraft where control moments are transmitted directly from pilot stick to the aircraft, in the case of rotorcraft control moments are transmitted indirectly from the pilot stick to the rotor through the swashplate mechanism to the blade pitch, causing the rotor to flap and thence transmitting moments to the aircraft. The main objective of this paper is to give a basic understanding of the mechanisms through which pilot cyclic inputs in lateral cyclic interacts with high-order rotor dynamics and results in destabilization of the helicopter roll motion. First, the explanation of the meaning of helicopters' higher-order rotor dynamics will be given.

1.1 Rotor multiblade modes and their couplings to the airframe modes

It is well-known that, in order to control the helicopter, the pilot applies cyclic inputs through his/her cyclic stick. These pilot inputs are applied at 1/rev-frequency to the rotor (i.e. frequency in the order of the rotor rotational frequency) through the swashplate mechanism.

Discussing on the blade flapping motion, this motion as seen from a frame of reference rotating with the blade, can be divided in three distinct time scales:

- Fast motions, corresponding to transients associated with the eigen frequency of the blade (angular frequency in the order of the rotor rotational frequency);
- Intermediate fast motion, corresponding to the steady state response of the blade to control inputs and body rotations;
- Slow motion, corresponding to the steady state response of the blade to variations of helicopter speed.

Since pilot control inputs depend mostly on aircraft body motions it would follow that these inputs would transmit to the rotor on the intermediate and slow time-scales. This would seem to be obvious at first sight, since these time-scales are clearly relevant for pilot and aircraft systems. The fast time-scale is more relevant for vibration, aero-elastic stability, etc. In accordance with this, the fast blade motions are usually neglected in the aircraft-pilot loop modelling, and the blade is assumed to respond instantaneously to control inputs, pitching motion and helicopter velocity. This is in fact an asymptotic approximation to the complete flapping behavior. However, such an approximation may be misleading. Low-frequency pilot inputs could generate high-frequency blade excitations. To understand this mechanism through which low frequency pilot input can be transmitted as high-frequency excitations to the helicopter body, one needs to consider the rotor behavior not in a rotating frame of reference rotating with the blades, but rather in the non-rotating frame of reference fixed to the helicopter body. It is therefore essential to first transform the rotor blade excitation, in the form of flap and lag motion from a rotating frame to a nonrotating (fixed) aircraft body frame. This may be done by applying the so-called multiblade (Coleman) transformation [4]. This transformation is a multiblade transformation which also takes into account the summation or cancelling effects due to different blades of the rotor. When the Coleman-transformation is applied, it appears that, in general, the transient blade motion splits into three levels bringing the concept of rotor modes as:

- a relatively low-frequency ‘regressing’ (called also regressive) rotor mode of frequency -1/rev lower than the isolated blade lead-lag frequency;
- an intermediate 'coning' (called also collective) rotor mode transferred directly without frequency shift from the rotating to the fixed frame, and
- a high frequency ‘advancing’ (called also progressive) mode of frequency +1/rev higher than the isolated blade lead-lag frequency.

The multiblade transformation is fundamental to comprehend the pilot-helicopter dynamics because through this, rotor blade excitations in the form of flap and lag motion are transferred back to the fixed airframe system as coning and cyclic (regressing and advancing) rotor modes. Under certain circumstances it is therefore conceivable that, for example, the regressing mode indeed becomes relevant for pilot-aircraft dynamics, despite the fact that it originates from the fast timescale motions in the rotating frame. If this happens to be the case, the regressing mode will probably couple to the aircraft body motion and become important in the pilot-aircraft loop. Concerning the lead-lag motion of the blade which will be of interest in this paper, the lead-lag mode transposes from the rotating system to the non-rotating system in:

- a collective (drive train) lead-lag mode where all the blades move simultaneously in the lead-lag direction with no shift of the rotor center of gravity;
- a progressing lead-lag mode corresponding to a high frequency whirling of the rotor center of gravity in the same direction as the rotor rotation;

- a regressing lead-lag mode corresponding to a low frequency whirling of the rotor center of gravity in the opposite direction as the rotor rotation (this is for a stiff-inplane rotor).

Well known problems involving couplings between the lead lag dynamics and the vehicle dynamics correspond to the "ground resonance" and "air resonance" instabilities. Ground resonance (GR) phenomenon involves a coupling between the regressing lead-lag mode and body roll motion that happens when the helicopter is grounded(see for example [1]-[3]).Air resonance (AR) phenomenon involves besides coupling between rotor regressing lead lag mode and body roll motion also couplings to the flapping motion. In both instabilities, a simple perturbation, e.g. caused by a pilot action on cyclic controls or a wind gust on the fuselage, can lead to instability appearing mainly in the aircraft roll motion. Ground and air resonance can be solved by increasing the damping levels. This may be accomplished through: 1) the use of lag dampers, however this results in extra weight, 2) introducing aeroelastic couplings in the rotor resulting in "damper less" configurations. To predict GR and AR one needs to transform frequency of the blade lead-lag mode from the rotating frame frequency (ω_ζ) to the nonrotating frame frequencies (i.e. regressing lead-lag mode $\left|\Omega-\omega_\zeta\right|$ and advancing lead-lag mode $\left|\Omega+\omega_\zeta\right|$) and represent these frequencies in a diagram giving the frequency of the lead-lag blade mode as seen in the nonrotating body frame as a function of rotor speed (Ω), see Fig. 1. Representing also the body roll and/ or pitch mode in this diagram one can determine regions of intersection of the regressing lead-lag mode to the body pitch and roll mode denoted as Air Resonance Region and Ground Resonance region in Fig. 1. Usually these intersections correspond to the area of regressing lead-lag mode so that in GR and AR only the regressing lead-lag mode is involved in the instability.

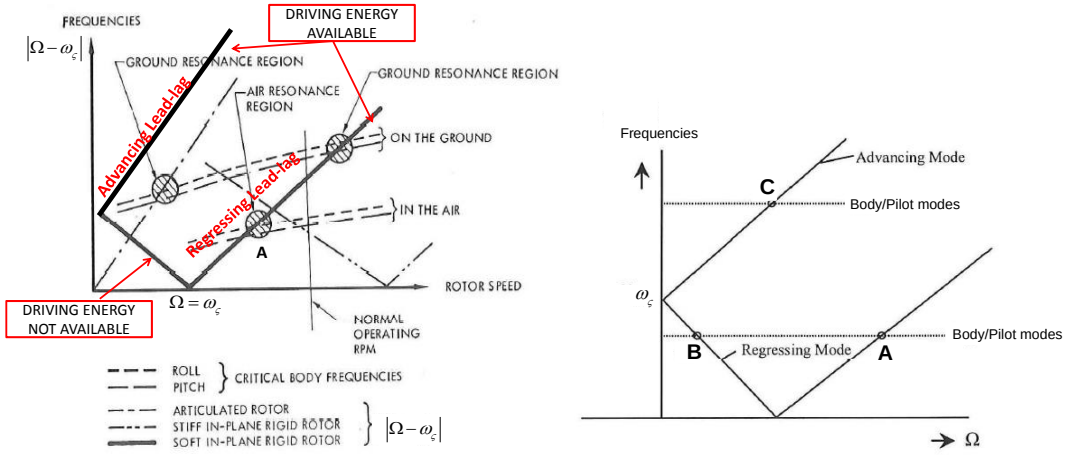

Fig. 1: Ground and Air resonance diagram at helicopters

1.2 Pilot involvement into the rotor multiblade modes

Based on flight experience with modern helicopters, it appears that the pilot can contribute to the ground and air resonances phenomena explained above changing their characteristics. For example, in 2008 reference [5] showed that an initial air resonance controller initially developed for the EC135 to alleviate the air resonance mode (the coupled regressing lead-lag -body roll mode) needed to be changed due to pilot involvement. More exactly, according to their study it appeared that, in the basic helicopter operation condition, air resonance was not

an issue for the pilots operating the EC135, the air resonance instability manifesting as a body roll oscillation which was existent but below the pilot perception level. However, when the helicopter was enhanced with an Attitude command/ Attitude Hold (ACAH) control system for flying attitude command or flight path following tasks, it became apparent that, increasing too much the roll rate feedback gain, drove unstable the air resonance mode. This time the oscillation was perceived by the pilot as an oscillatory ringing in the helicopter roll response. In order to damp the air resonance mode when rate feedback was used, an air resonance controller needed to be developed which effectively damped the coupled body-roll air resonance mode, independently from the main flight control system.

Other examples of pilot inputs interacting with the first vertical and lateral fuselage bending modes through the Automatic Flight Control System (AFCS) were reported for the CH-46D/E Sea Knight, the SH-60B Seahawk, and the CH-53E Super Stallion helicopters with external loads [6]. In these cases, the pilot inputs manifested as involuntarily (uncommanded) controls demonstrating that instabilities a là "Pilot Assisted Oscillations" (PAOs) were occurring for these vehicles. Pilot assisted oscillations (PAO) phenomena are a class of Rotorcraft-Pilot Couplings (RPC), i.e. instabilities originating from adverse couplings in the pilot-vehicle system (PVS). RPCs can manifest as:

- PIOs -Pilot Induced Oscillations - which occur when the pilot inadvertently causes divergent oscillations by applying control inputs which are essentially in the wrongdirection, or have a significant phase lag with respect to the aircraft/rotorcraft response. High gain tasks, long time delays introduced by the pilot while controlling the aircraft or changes in the pilot control behavior introduced by FCS and control interfaces can all be the cause of a PIO,
- PAOs -Pilot Assisted Oscillations - are higher frequency phenomenon related to involuntary control inputs given from the pilot, which may destabilize the aircraft.

During ARISTOTEL project in Europe ([7]-[9], [15]) PAOs were revealed in the simulator for a Bo-105 helicopter during the roll step maneuver [9]. In the roll step maneuver the pilot was flying through a series of gates traversing the runway from one side to the other in a specified distance and initial velocity.

When flying the roll step maneuver from an initial velocity of 80 knots with two test pilots it was observed that while one pilot triggered the PAO instability in the roll axis, the other pilot was able to complete maneuver.

At this point it should be underlined that all PAO instabilities discussed in the literature of specialty related to the low-frequency regressing lag mode that coupled to the roll and pitch motions through the pilot dynamics.

However, more recently, research published by Tod, Pavel et. al [10] showed that when the pilot 'stiffens' his arm in order to control a high precision manoeuvre, the advancing lag mode can become unstable.

This is an interesting result as advancing lead-lag mode is a much higher-frequency order mode than the airframe modes and should be well separated from the pilot-vehicle interactions. Trying to understand why the advancing mode was excited by the pilot and become unstable, the authors showed that a pilot stiffening his/her arm to fly a manoeuvre results in a pilot mode that intersects the advancing lead lag mode branch of Fig. 1. Also, the stiffer pilot arm gives a more strongly coupled flap-lag motion enabling the "pumping" of energy from pilot to the rotor and back.

The remaining part of the paper will understand the physical mechanism through which the pilot excites the advancing lead lag mode and, contrary to what usually believed, drives unstable the high frequency advancing lead lag mode.

2. THE MECHANISM OF PILOT DESTABILIZATION OF HELICOPTER ROTOR LEAD-LAG MODES

In order to understand the mechanism through which the lateral PAO instability evolves one should represent the modes involved in the instability and, see Fig. 2 adapted from ref. [11]. The cycle starts when a lateral cyclic pitch control is given by the pilot. Through AFCS, the pilot input is transmitted to the swashplate and then to the blade as cyclic pitch dynamics (main rotor MR pitch dynamics θ_{1C} and θ_{1S} for the cosine and sine terms). This will modify the angle of attack of each blade, inducing a cyclic flapping motion (main rotor MR flap dynamics β_{1C} and β_{1S} for the cosine and sine terms). However, as blade flaps it also lags and therefore the blade will also have a cyclic lag (main rotor MR lag dynamics ζ_{1C} and ζ_{1S} for the cosine and sine terms). This will move the rotor center of mass from its axis of rotation, which will further induce vibratory roll and pitch moments in the fuselage, that are transmitted as lateral and longitudinal vibrations in the cockpit and to the pilot seat. The pilot will react to these vibrations through his/her "biodynamics", i.e. will apply involuntarily cyclic control stick inputs and the above-cycle is again repeated.

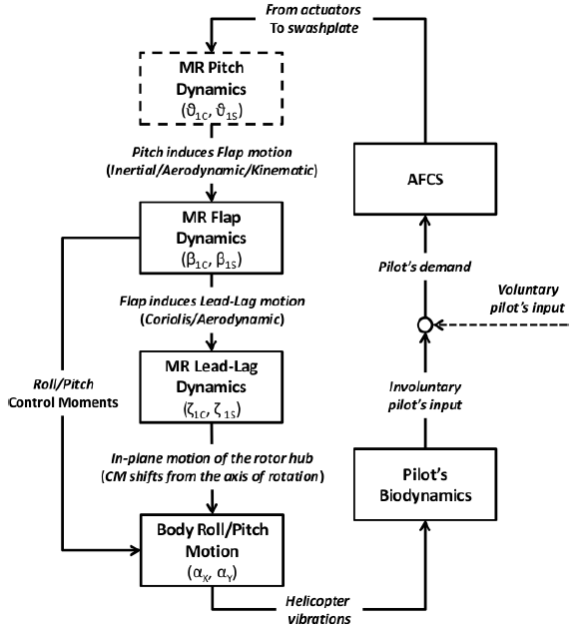

Fig. 2: The lateral PAO mechanism of instability at helicopters (adapted from ref. [11])

In order to verify the lateral PAO instability mechanism presented above the present paper will use a physical approach. The main idea in a physical approach is that in a self excited system there is an energy flow which enables the degrees of freedom involved in the instability to pump energy into each other (refs [12]-[14]). Using this energetic approach to the problem it follows that:

- if there are degrees of freedom which mutually pump energy into each other, this indicates the possibility of dynamic instability;
- any external excitations (coupling terms) in phase with the velocity of the degree of freedom considered will pump energy into that DOF;
- a harmonic force acting on a vibrating system of the same frequency produces work on the system if the force is in phase with the velocity of the vibration.

Consider a simplified model for the rotor-aircraft as seen in Fig. 3. The model consists of a constant speed shaft (angular velocity ψ) which may translate longitudinally and laterally w.r.t. an inertial frame. A hub is connected to the shaft by means of a spring K_ζ, so that the hub may have a variable angular velocity $\Omega+\dot{\zeta}$. To the hub is attached a massless beam with a concentrated mass m at its end. In order to balance the average centrifugal force, a counterweight is attached to the shaft. For the moment, the blade flapping motion is not included in the model as point A of Fig. 1 is not giving explicitly the importance of flap motion in AR problem. Looking at Fig. 3, the angular velocity of the blade is:

$$\underline{\omega}_{bl} = (0,0,\Omega+\dot{\zeta})\{\underline{E}_{bl}\} \tag{1}$$

where $\{\underline{E}_{bl}\} = \{\underline{i}_{bl}, \underline{j}_{bl}, \underline{k}_{bl}\}^T$ is the row of unit vectors defining the reference frame of the blade ($\underline{i}_{bl}$ is the unit vector in x direction, $\underline{j}_{bl}$ is the unit vector in y direction and $\underline{k}_{bl}$ is the unit vector in z direction).

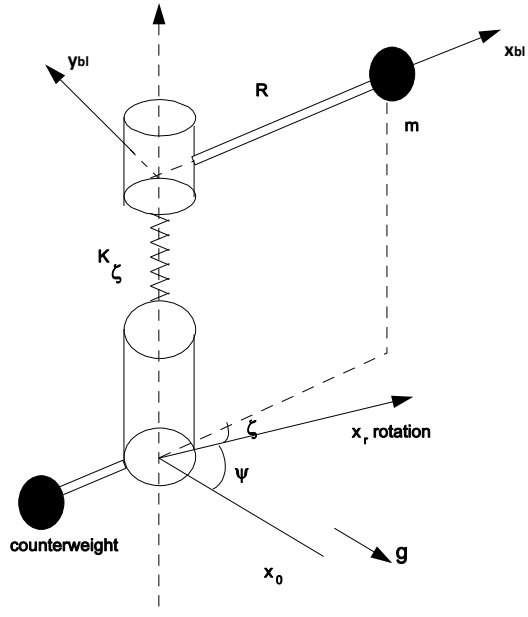

Fig. 3: Rotor-body model for helicopter roll axis motion

The absolute displacement of the blade is then:

$$\underline{r} = R(1,0,0)\{\underline{E}_{bl}\} \tag{2}$$

The absolute velocity:

$$\dot{\underline{r}} = R(1,0,0)\{\dot{\underline{E}}_{bl}\} = R(1,0,0)[\omega_{blx}]\{\underline{E}_{bl}\} \tag{3}$$

where $[\omega_{blx}]$ represents the matrix time derivative of the unit vector $\{\dot{\bar{E}}\} = \begin{bmatrix} 0 & r & -q \\ -r & 0 & p \\ q & -p & 0 \end{bmatrix}\{\bar{E}\}$

that is in our case: $[\omega_{blx}] = \begin{bmatrix} 0 & \Omega+\dot{\zeta} & 0 \\ -(\Omega+\dot{\zeta}) & 0 & 0 \\ 0 & 0 & 0 \end{bmatrix}$. The absolute acceleration of the blade is:

$$\underline{\ddot{r}} = R(1,0,0)[\dot{\omega}_{bl}]\{\underline{E}_{bl}\} + R(1,0,0)[\omega_{blx}]^2\{\underline{E}_{bl}\} = R\left(-(\Omega+\dot{\varsigma})^2, \ddot{\varsigma}, 0\right)\{\underline{E}_{bl}\} \tag{4}$$

The force due to the "lead-lagging" mass on the hub is then:

$$\underline{F}_{bl} = (F_x, F_y, 0)\{\underline{E}_{bl}\} \tag{5}$$

According to D'Alembert principle[1], this means the inertial forces:

$$\begin{aligned} F_x &= mR(\Omega+\dot{\varsigma})^2 \\ F_y &= -mR\ddot{\varsigma} \end{aligned} \tag{6}$$

Lead-lag moment equation:

$$-F_y R + K_\varsigma \varsigma = 0 \tag{7}$$

$$\ddot{\varsigma} + \omega_\varsigma{}^2 \varsigma = 0 \tag{8}$$

with $\omega_\varsigma = \sqrt{\frac{K_\varsigma}{mR^2}}$. The force on the shaft, taking into account the extra counter-weight is:

$$\underline{F}_r = (F_x, F_y, 0)[\varsigma]\{\underline{E}_r\} - mR\Omega^2(1,0,0)\{\underline{E}_r\} \tag{9}$$

with $[\varsigma] = \begin{bmatrix} \cos\varsigma & \sin\varsigma & 0 \\ -\sin\varsigma & \cos\varsigma & 0 \\ 0 & 0 & 1 \end{bmatrix}$ the rotation matrix from $\{\underline{E}_r\}$ to $\{\underline{E}_{bl}\}$ ($\{\underline{E}_{bl}\} = [\varsigma]\{\underline{E}_r\}$).

Linearizing force $\underline{F}_r$ it follows that:

$$\begin{array}{lccc} \underline{F}_r \approx^{\text{linearized}} mR & \left(2\Omega\dot{\varsigma}, \right. & \Omega^2\varsigma - \ddot{\varsigma}, & \left. 0 \right) \{\underline{E}_r\} \\ & \uparrow & \uparrow & \uparrow \\ & \text{Coriolis} & \text{Centrifugal} & \text{Inertial} \end{array} \tag{10}$$

2.1 Case A - Pilot mode interacting with regressing lead-lag mode (vertical branch)

Firstly, consider the AR situation as represented by point A in Fig. 1 and assume that the values of the eigen frequencies are:

$$\begin{aligned} \omega_\varsigma &= \frac{1}{2}\Omega \\ \omega_{sh} &= \frac{1}{2}\Omega \end{aligned} \tag{11}$$

Assume an oscillatory motion:

$$\varsigma = \varsigma_0 \cos\left(\omega_\varsigma t\right) = \varsigma_0 \cos\left(\frac{1}{2}\Omega t\right) = \varsigma_0 \cos\left(\frac{\psi}{2}\right) \tag{12}$$

It follows that the lag velocity and lag accelerations are:

$$\dot{\varsigma} = -\varsigma_0\omega_\varsigma \sin\left(\omega_\varsigma t\right) = -\frac{1}{2}\varsigma_0\Omega\sin\left(\frac{\psi}{2}\right) \tag{13}$$

[1] D'Alembert principle allows converting dynamic problems in static ones. Typical usage of this principle consists of representing the statement of Newton's second law F=ma by an "inertial load" equal to ma, but directed opposite to the acceleration, a.

$$\ddot{\varsigma} = -\varsigma_0 \omega_\varsigma^2 \cos\left(\omega_\varsigma t\right) = -\frac{1}{4}\varsigma_0 \Omega^2 \cos\left(\frac{\psi}{2}\right) \tag{14}$$

First, describe the lead-lag motion as an external excitation for the shaft. The effective forces on the hub due to the blade lead-lag motion can be found by substituting (13) and (14) into equation (10):

$$\begin{aligned} F_{xr} &= 2mR\Omega\dot{\varsigma} = -mR\Omega^2\varsigma_0 \sin\left(\frac{\psi}{2}\right) \quad \text{(Coriolis)} \\ F_{yr} &= mR\left(\Omega^2\varsigma - \ddot{\varsigma}\right) = \frac{5}{4}mR\Omega^2\varsigma_0 \cos\left(\frac{\psi}{2}\right) \quad \text{(cf + inertia)} \end{aligned} \tag{15}$$

Since one investigates the system at resonance, and because the external lead-lag motion excites the shaft in a resonant point, it follows that the blade lead-lag motion gives rise to a shaft motion 90 deg phased w.r.t. the lead-lag motion. Using (12) and (15), the motion of one blade over 4 periods and the force on the shaft can be represented (each lead-lag cycle takes two revolutions) as shown in Fig. 4.

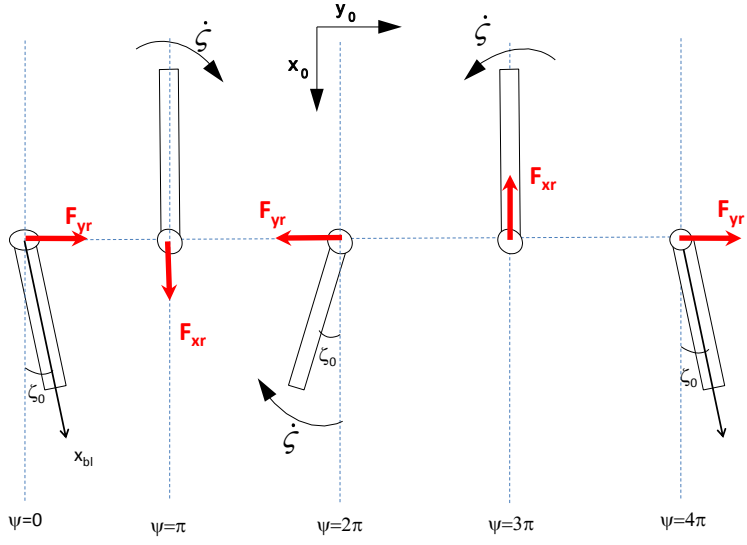

Fig. 4: Lead-lag motion of one blade as external excitation for the shaft and the corresponding force on the shaft- Case A

One can see that, regarding the forcing terms acting on the shaft, a force will be exerted on the shaft to the right. One revolution later, at $\psi=2\pi$ maximum lag occurs with an attendant force on the shaft to the left, etc. When desired, this may be also checked by substituting $\zeta(\psi)$ into the equations of motion. Concluding, there is a "rotating" force acting on the shaft, against the rotor direction of rotation. Secondly, describe the shaft motion as an external excitation for the blades. Assume that the shaft can move only longitudinally (direction x_0), being excited in its eigen frequency $\omega_{sh} = (1/2)\Omega$. The blades will move up and down with the shaft with acceleration $\ddot{x}_{sh}$. Looking at (12), the shaft longitudinal displacement will be:

$$x_{sh} = x_{sh0} \cos\left(\omega_{sh} t\right) = x_{sh0} \cos\left(\frac{\psi}{2}\right) \tag{16}$$

D'Alembert principle will be used next to determine the force on blade due to the shaft motion:

$$f = -f_0 \cos\left(\frac{\psi}{2}\right) \tag{17}$$

and the motion of the shaft during 4 periods is now as represented in Fig. 5.

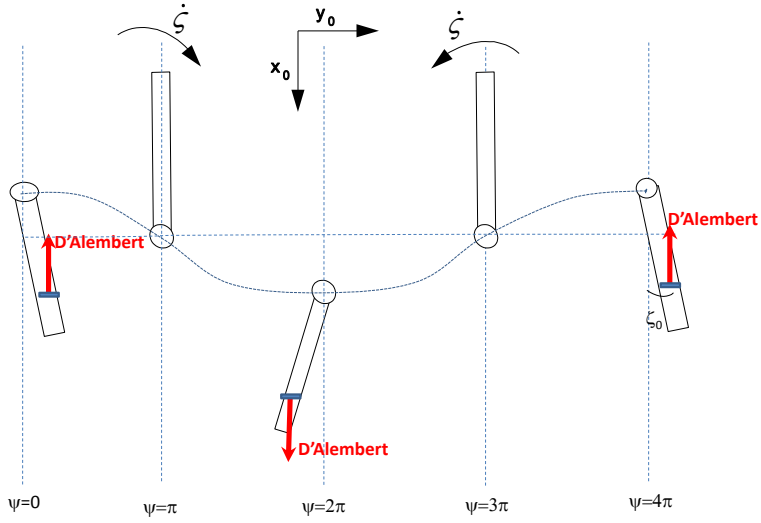

Fig. 5: Longitudinal shaft motion as external excitation for the blade and the corresponding force on the blade – Case A

Furthermore, it appears that:

- Fxr is in phase with $\dot{x}_{sh}$, thus energy input goes in the shaft.
- An extra lead-lag moment as a result of the shaft acceleration is out of phase with $\dot{\varsigma}$, so there is no energy input from the shaft to the blade.

The extra lead-lag moment due to the longitudinal shaft motion can be calculated as:

$$M = -fR\sin(\psi+\varsigma) \overset{\text{linearized}}{\approx} f_0 R\cos\left(\frac{\psi}{2}\right)(\sin\psi+\varsigma\cos\psi) = f_0 R\cos\left(\frac{\psi}{2}\right)\times\left(\sin\psi+\varsigma_0\cos\left(\frac{\psi}{2}\right)\cos\psi\right) =$$
$$f_0 R\left[\frac{1}{2}\sin\left(\frac{3\psi}{2}\right)+\frac{1}{2}\sin\left(\frac{\psi}{2}\right)\right]+f_0\varsigma_0 R\left(1+2\cos\psi+\cos 2\psi\right) \tag{18}$$

Equation (18) does not contain any component in phase with lag velocity (13).

Assume now that the shaft can move only laterally (direction y0). The shaft lateral displacement will be:

$$x_{sh} = x_{sh0}\sin(\omega_{sh}t) = x_{sh0}\sin\left(\frac{\psi}{2}\right) \tag{19}$$

The lateral force on blade due to the shaft motion is given according to D'Alembert principle as:

$$f = f_0\sin\left(\frac{\psi}{2}\right) \tag{20}$$

The lateral shaft motion during 4 periods can be represented now as seen in Fig. 6.

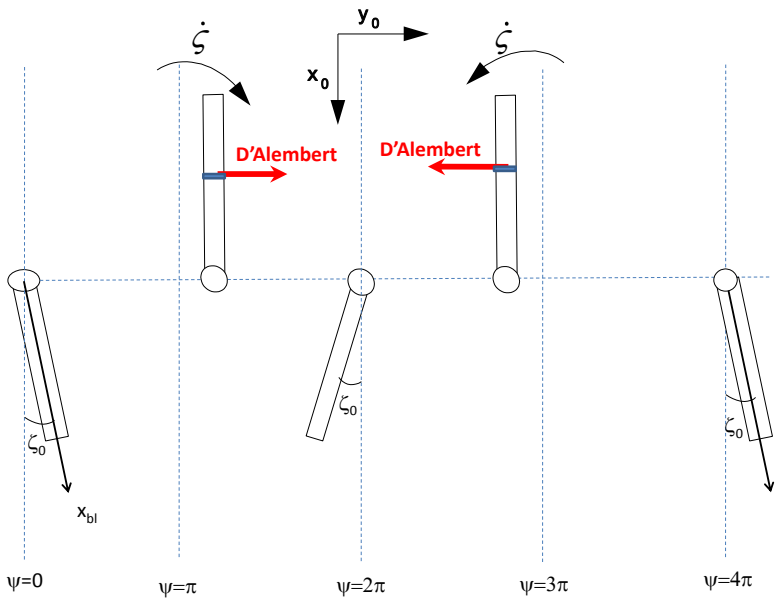

Fig. 6: Lateral shaft motion as external excitation for the blade and the corresponding force on the blade – Case A

It can be seen that:

- F_{yr} is in phase with $\dot{y}_{sh}$, so energy input goes in the shaft.
- An extra lead- lag moment as a result of the shaft acceleration is in phase with $\dot{\varsigma}$, thus there is energy input from the shaft to the blades

The extra lead-lag moment due to the lateral shaft motion can be calculated as:

$$M = fR\cos(\psi+\varsigma) \overset{\text{linearized}}{\approx} f_0 R\sin\left(\frac{\psi}{2}\right)(\cos\psi-\varsigma\sin\psi) = f_0 R\sin\left(\frac{\psi}{2}\right)\times\left(\cos\psi-\varsigma_0\cos\left(\frac{\psi}{2}\right)\sin\psi\right) = f_0 R\left[\frac{1}{2}\sin\left(\frac{3\psi}{2}\right)-\frac{1}{2}\sin\left(\frac{\psi}{2}\right)\right]-f_0\varsigma_0 R\left(\frac{1}{4}-\frac{1}{4}\cos 2\psi\right) \quad (21)$$

In this case, relation (21) does contain a component in phase with lag velocity (13). This shows that, in ground resonance (represented as an intersection point between shaft and blade lead-lag frequency in the $|\Omega-\omega_\varsigma|$ diagram, the lateral shaft motion combines with blade lead-lag motion. Consider next that there is an extra pilot force exciting the lag mode in the same direction. In this case, the D'Alembert force becomes:

$$f = f_0\sin\left(\frac{\psi}{2}\right)+f_{pilot} \quad (22)$$

The extra lead-lag moment due to the lateral shaft motion can be calculated as:

$$M = fR\cos(\psi+\varsigma) \overset{\text{linearized}}{\approx} f_0 R\sin\left(\frac{\psi}{2}\right)(\cos\psi-\varsigma\sin\psi)+f_{pilot}R(\cos\psi-\varsigma\sin\psi) = f_0 R\sin\left(\frac{\psi}{2}\right)\times\left(\cos\psi-\varsigma_0\cos\left(\frac{\psi}{2}\right)\sin\psi\right)-f_{pilot}R\times\left(\cos\psi-\varsigma_0\cos\left(\frac{\psi}{2}\right)\sin\psi\right) = f_0 R\left(\frac{1}{2}\sin\left(\frac{3\psi}{2}\right)-\frac{1}{2}\sin\left(\frac{\psi}{2}\right)\right)-f_0\varsigma_0 R\left(\frac{1}{4}-\frac{1}{4}\cos 2\psi\right)-f_{pilot}R\cos\psi-f_{pilot}R\varsigma_0\left(\sin\left(\frac{3\psi}{2}\right)+\sin\left(\frac{\psi}{2}\right)\right) \quad (23)$$

The lead-lag moment (23) due to the lateral shaft motion contains two components in phase with lag velocity (13), one introduced by the shaft motion and the other introduced by the pilot force. This corresponds indeed with results acknowledged by other references [11, 15].

2.2 Case B- Body/Pilot mode interacting with regressing lead-lag mode (horizontal branch)

Consider next that the crossing of the shaft eigen frequency with the regressing lead-lag mode occurs in point B, see Fig. 1. Assume in this case that the eigen frequencies have the form:

$$\begin{aligned} \omega_{\varsigma} &= 2\Omega \\ \omega_{\mathrm{sh}} &= \Omega \end{aligned} \tag{24}$$

The lead-lag motion becomes:

$$\varsigma = \varsigma_0 \cos\left(\omega_{\varsigma} t\right) = \varsigma_0 \cos 2\psi \tag{25}$$

and the blade lead lag velocity and acceleration are:

$$\dot{\varsigma} = -\varsigma_0 \omega_{\varsigma} \sin\left(\omega_{\varsigma} t\right) = -2\varsigma_0 \Omega \sin 2\psi \tag{26}$$

$$\ddot{\varsigma} = -\varsigma_0 \omega^2{}_{\varsigma} \cos\left(\omega_{\varsigma} t\right) = -4\varsigma_0 \Omega^2 \cos 2\psi \tag{27}$$

Following the same procedure as above and describing first the lead-lag motion as an external excitation for the shaft, one can determine the effective forces on the hub due to the blade lead-lag motion as:

$$\begin{aligned} \mathrm{F_{xr}} &= 2\mathrm{mR}\Omega\dot{\varsigma} = -4\mathrm{mR}\Omega^2\varsigma_0 \sin 2\psi \quad \text{(Coriolis)} \\ \mathrm{F_{yr}} &= \mathrm{mR}\left(\Omega^2\varsigma - \ddot{\varsigma}\right) = 5\mathrm{mR}\Omega^2\varsigma_0 \cos 2\psi \quad \text{(Cf.+Inertia)} \end{aligned} \tag{28}$$

The first harmonic of the hub forces due to the blade lead-lag motion as seen by the shaft can be extracted by projecting these forces onto the shaft system of reference x0y0z0 as see in Fig. 7.

$$\begin{aligned} \mathrm{F_{x0}} &= \mathrm{F_{xr}} \cos\psi - \mathrm{F_{yr}} \sin\psi = \frac{1}{2}\mathrm{mR}\Omega^2\varsigma_0 \sin\psi - \frac{9}{2}\mathrm{mR}\Omega^2\varsigma_0 \sin 3\psi \\ \mathrm{F_{y0}} &= \mathrm{F_{xr}} \sin\psi + \mathrm{F_{yr}} \cos\psi = \frac{1}{2}\mathrm{mR}\Omega^2\varsigma_0 \cos\psi + \frac{9}{2}\mathrm{mR}\Omega^2\varsigma_0 \cos 3\psi \end{aligned} \tag{29}$$

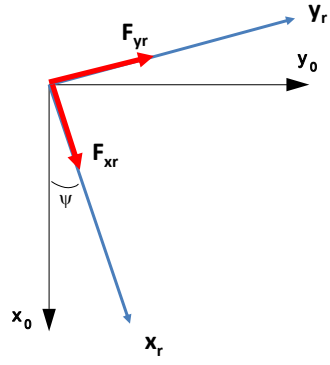

Fig. 7: Projection of hub forces induced by lead-lag motion on the shaft

Using (25) and (28), the 1st harmonic on the shaft can be represented as seen in Fig. 8.

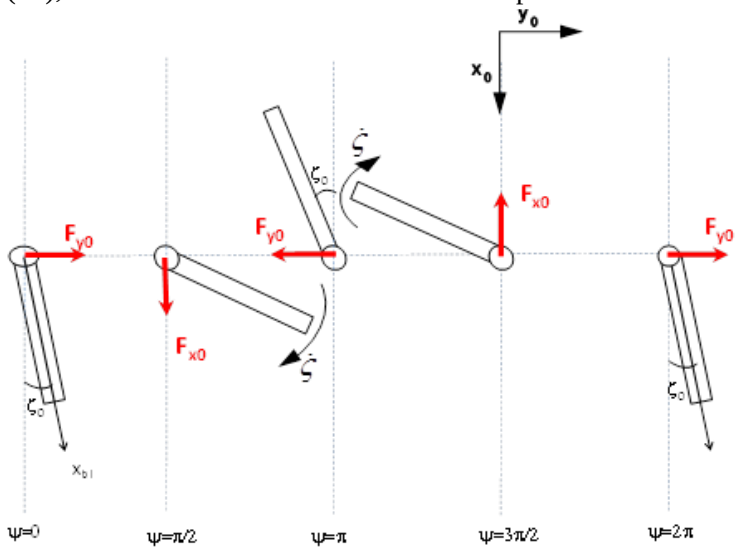

Fig. 8: Lead-lag motion of one blade as external excitation for the shaft and the corresponding force on the shaft – Case B

Describe next the shaft motion as an external excitation for the blades. Assume that the shaft can move only longitudinally (direction x_0), being excited in its eigen frequency $\omega_{sh} = \Omega$. The blades will move up and down with the shaft with an acceleration $\ddot{x}_{sh}$. Looking at (25), the shaft longitudinal displacement will be:

$$x_{sh} = x_{sh0}\cos(\omega_{sh} t) = x_{sh0}\cos\psi \tag{30}$$

The force on blade due to the shaft motion is according to D'Alembert principle:

$$f = -f_0\cos\psi \tag{31}$$

and the motion of the shaft during one rotor revolution is represented as seen in Fig. 9.

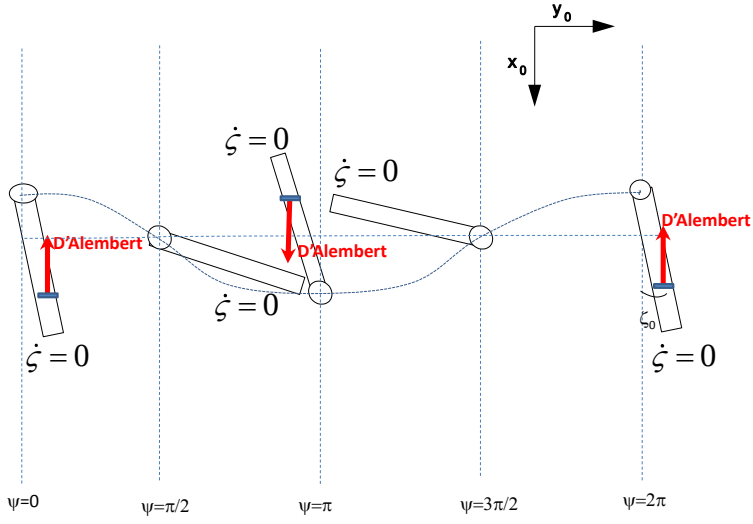

Fig. 9: Longitudinal shaft motion as external excitation for the blade and the corresponding force on the blade – Case B

The extra lead-lag moment due to the longitudinal shaft motion can be calculated as:

$$M = -fR\sin(\psi+\varsigma) \overset{\text{linearized}}{\approx} f_0 R\cos(\psi)(\sin\psi+\varsigma\cos\psi) = f_0 R\cos(\psi)\times$$
$$(\sin\psi+\varsigma_0\cos(2\psi)\cos\psi) = f_0 R\frac{1}{2}\sin 2\psi + f_0\varsigma_0 R\left(\frac{1}{2}\cos 3\psi+\frac{1}{2}\cos\psi\right) \quad (32)$$

It can be seen that (32) is out of phase with lag velocity (26), thus there is no energy passing from the shaft to the blades.

Also, from (43) and (30), one can see that Fx_0 is out of phase with $\dot{x}_{sh}$, thus no energy input goes from the blades to the shaft.

Assuming next that the shaft can move only laterally (direction y0) and following the procedure explained above, the shaft lateral displacement can be described as:

$$x_{sh} = x_{sh0}\sin(\omega_{sh}t) = x_{sh0}\sin\psi \quad (33)$$

The force on blade due to the shaft motion is according to D'Alembert principle:

$$f = -f_0\sin\psi \quad (34)$$

and the lateral motion of the shaft during one rotor revolution is represented as seen in Fig. 10.

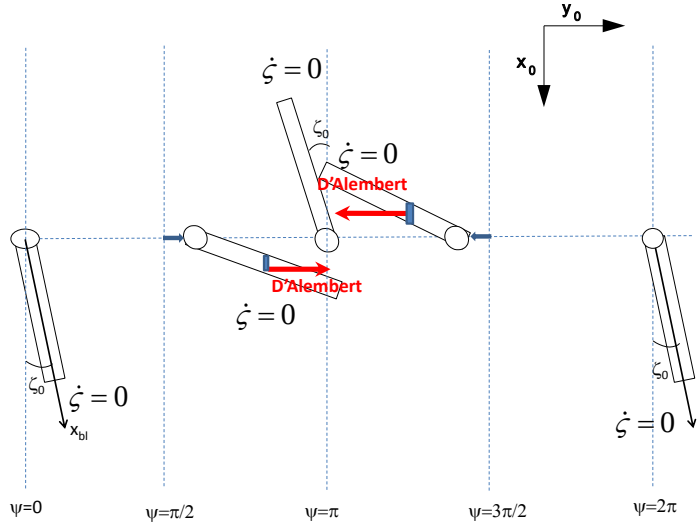

Fig. 10: Lateral shaft motion as external excitation for the blade and the corresponding force on the blade- Case B

The extra lead-lag moment due to the lateral shaft motion can be calculated as:

$$M = fR\cos(\psi+\varsigma) \overset{\text{linearized}}{\approx} f_0 R\sin\psi(\cos\psi+\varsigma\sin\psi) = f_0 R\sin\psi\times$$
$$(\cos\psi-\varsigma_0\cos(2\psi)\sin\psi) = f_0 R\frac{1}{2}\sin 2\psi - f_0\varsigma_0 R\left(\frac{1}{2}\cos 2\psi-\frac{1}{4}-\frac{1}{4}\cos 4\psi\right) \quad (35)$$

Looking at (35) it appears that this is also out of phase with lag velocity (26), thus there is no energy passing from the shaft to the blades. Also, from (43) and (33) one can see that Fy0 is in phase with $\dot{x}_{sh}$, thus there is energy input going from the blades to the shaft. However, as no energy goes back from the shaft to the blades, this part of the regressing

lead-lag mode branch is not dangerous for air/ground resonance instability as driving energy is not available. Consider next that there is an extra pilot force exciting the lag mode in the same direction. In this case, the D'Alembert force becomes:

$$f = -f_0 \sin\psi - f_{pilot} \tag{36}$$

The extra lead-lag moment due to the lateral shaft motion can be calculated as:

$$\begin{aligned} M &= fR\cos(\psi+\varsigma) \overset{\text{linearized}}{\approx} f_0 R\sin\psi(\cos\psi+\varsigma\sin\psi)+f_{pilot}R(\cos\psi+\varsigma\sin\psi)= \\ &f_0 R\sin\psi(\cos\psi-\varsigma_0\cos(2\psi)\sin\psi)+f_{pilot}R(\cos\psi-\varsigma_0\cos(2\psi)\sin\psi) \\ &= f_0 R\frac{1}{2}\sin 2\psi - f_0\varsigma_0 R\left(\frac{1}{2}\cos 2\psi-\frac{1}{4}-\frac{1}{4}\cos 4\psi\right)+f_{pilot}R\cos\psi-f_{pilot}R\varsigma_0\left(\frac{1}{2}\sin(3\psi)-\frac{1}{2}\sin\psi\right) \end{aligned} \tag{37}$$

The lead-lag moment (23) due to the lateral shaft motion does not contain any component in phase with lag velocity, neither from the shaft motion no from the pilot force.

2.3 Case C- Body/Pilot mode interacting with advancing lead-lag mode

Next, consider that the crossing of the shaft eigen frequency with the advancing lead-lag mode occurs in point C, see Fig. 1. In these case one can assume the eigen frequencies as:

$$\begin{aligned} \omega_\varsigma &= \Omega \\ \omega_{sh} &= 2\Omega \end{aligned} \tag{38}$$

The assumed oscillatory lead-lag motion is then:

$$\varsigma = \varsigma_0\cos(\omega_\varsigma t) = \varsigma_0\cos\psi \tag{39}$$

And the blade lead lag velocity and acceleration are:

$$\dot{\varsigma} = -\varsigma_0\omega_\varsigma\sin(\omega_\varsigma t) = -\varsigma_0\Omega\sin\psi \tag{40}$$

$$\ddot{\varsigma} = -\varsigma_0\omega_\varsigma^2\cos(\omega_\varsigma t) = -\varsigma_0\Omega^2\cos\psi \tag{41}$$

Describing first the lead-lag motion as an external excitation for the shaft, one can determine the effective forces on the hub due to the blade lead-lag motion as:

$$\begin{aligned} F_{xr} &= 2mR\Omega\dot{\varsigma} = -2mR\Omega^2\varsigma_0\sin\psi \quad \text{(Coriolis)} \\ F_{yr} &= mR(\Omega^2\varsigma-\ddot{\varsigma}) = 2mR\Omega^2\varsigma_0\cos\psi \quad \text{(Cf.+Inertia)} \end{aligned} \tag{42}$$

The first harmonic of the hub forces due to the blade lead-lag motion as seen by the shaft can be extracted by projecting these forces onto the shaft system of reference $x_0y_0z_0$ as seen in Fig. 11.

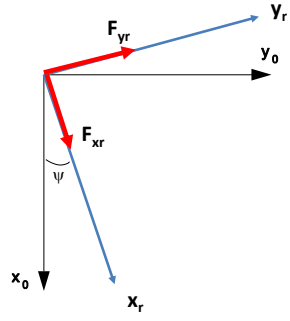

Fig. 11: Projection of hub forces induced by lead-lag motion on the shaft

Looking at Fig. 11 it follows that:

$$\begin{aligned} F_{x0} &= F_{xr}\cos\psi - F_{yr}\sin\psi = \frac{1}{2}mR\Omega^2\varsigma_0\sin\psi - \frac{9}{2}mR\Omega^2\varsigma_0\sin 3\psi \\ F_{y0} &= F_{xr}\sin\psi + F_{yr}\cos\psi = \frac{1}{2}mR\Omega^2\varsigma_0\cos\psi + \frac{9}{2}mR\Omega^2\varsigma_0\cos 3\psi \end{aligned} \tag{43}$$

The hub forces due to the blade lead-lag motion as seen by the shaft are obtained using (43) and Fig. 7 as:

$$\begin{aligned} F_{x0} &= F_{xr}\cos\psi - F_{yr}\sin\psi = -2mR\Omega^2\varsigma_0\sin 2\psi \\ F_{y0} &= F_{xr}\sin\psi + F_{yr}\cos\psi = 2mR\Omega^2\varsigma_0\cos 2\psi \end{aligned} \tag{44}$$

Using (39) and (44), the shaft forces and the blade motion can be represented as seen in Fig. 12.

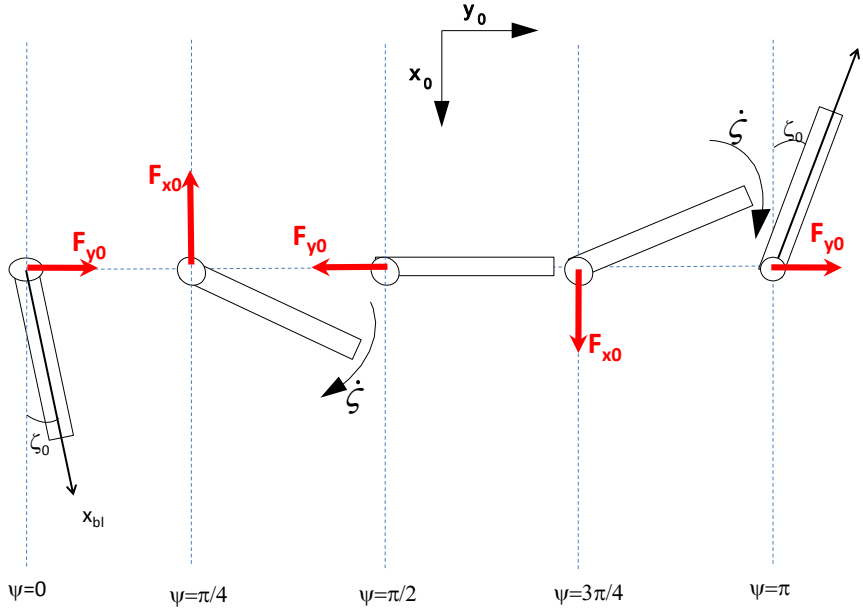

Fig. 12: Lead-lag motion of one blade as external excitation for the shaft and the corresponding force on the shaft – Case C

Describe next the shaft motion as an external excitation for the blades. Assume that the shaft can move only longitudinally (direction x0), being excited in its eigen frequency $\omega_{sh} = \Omega$. The blades will move up and down with the shaft with an acceleration $\ddot{x}_{sh}$. Looking at (39), the shaft longitudinal displacement will be:

$$x_{sh} = x_{sh0}\cos(\omega_{sh}t) = x_{sh0}\cos 2\psi \tag{45}$$

The force on blade due to the shaft motion is according to D'Alembert principle:

$$f = -f_0\cos 2\psi \tag{46}$$

and the motion of the shaft during one rotor revolution is represented as seen in Fig. 13. The extra lead-lag moment due to the longitudinal shaft motion can be calculated as:

$$M = -fR\sin(\psi+\varsigma) \overset{\text{linearized}}{\approx} -f_0R\cos(2\psi)(\sin\psi+\varsigma\cos\psi) = -f_0R\cos(2\psi)(\sin\psi+\varsigma_0\cos^2\psi) = -f_0R\left(\frac{1}{2}\sin 3\psi - \frac{1}{2}\sin\psi\right) - f_0\varsigma_0R\left(\frac{1}{4}+\frac{1}{2}\cos 2\psi+\frac{1}{4}\cos 4\psi\right) \quad (47)$$

One can see that (47) is out of phase with lag velocity (40), thus there is no energy passing from the shaft to the blades. Also, from (45) and (44), one can see that Fx_0 is in phase with $\dot{x}_{sh}$, thus energy input goes from the blades to the shaft.

Assuming next that the shaft can move only laterally (direction y_0) and following the procedure explained above, the shaft lateral displacement can be described as:

$$x_{sh} = x_{sh0}\sin(\omega_{sh}t) = x_{sh0}\sin 2\psi \quad (48)$$

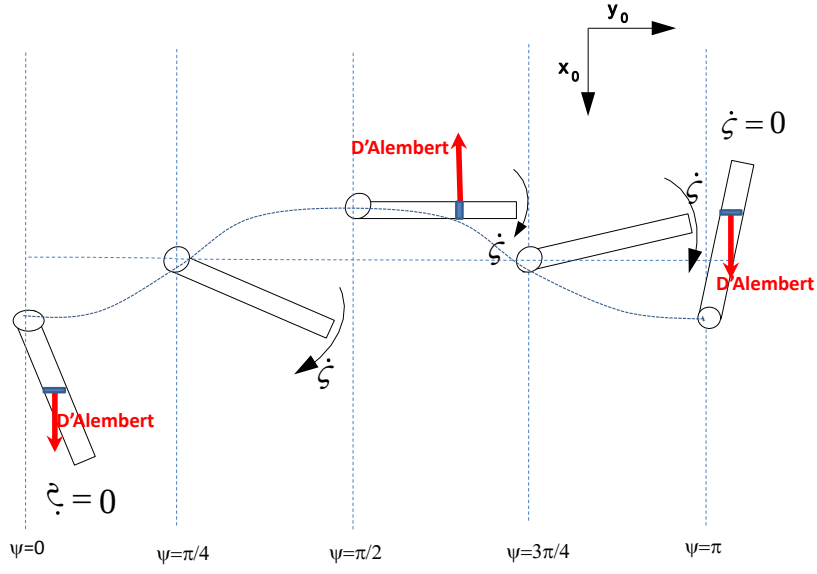

Fig. 13: Longitudinal shaft motion as external excitation for the blade and the corresponding force on the blade – Case C

The force on blade due to the shaft motion is according to D'Alembert principle:

$$f = -f_0\sin 2\psi \quad (49)$$

and the lateral motion of the shaft during one rotor revolution is represented as seen in Fig. 14. The extra lead-lag moment due to the lateral shaft motion can be calculated as:

$$M = fR\cos(\psi+\varsigma) \overset{\text{linearized}}{\approx} f_0R\sin 2\psi(\cos\psi-\varsigma\sin\psi) = f_0R\sin 2\psi(\cos\psi-\varsigma_0\sin\psi\cos(2\psi)) = f_0R\left(\frac{1}{2}\sin 3\psi+\frac{1}{2}\sin\psi\right) - f_0\varsigma_0R\left(\frac{1}{4}-\frac{1}{4}\cos 2\psi\right) \quad (50)$$

One can see that (50) contains one component out of phase with lag velocity (40), thus there is no energy passing from the shaft to the blades.
Therefore, the advancing lead-lag mode branch of Fig. 1, although contains driving energy, it does not close the vicious circle of energy flow from the blade lead-lag motion to the shaft motion and back.

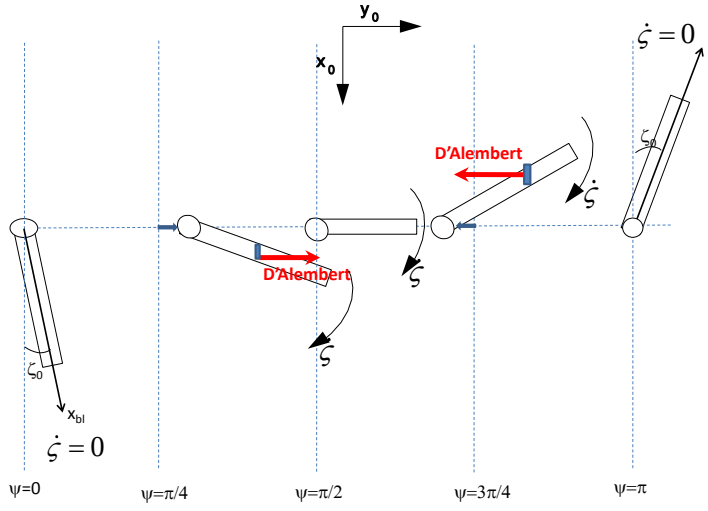

Fig. 14: Lateral shaft motion as external excitation for the blade and the corresponding force on the blade – Case C

However, the above case does not consider the extra pilot force exciting the lag mode. In this case, the D'Alembert force becomes:

$$f = -f_0 \sin 2\psi - f_{pilot} \tag{51}$$

The extra lead-lag moment due to the lateral shaft motion can be calculated as:

$$\begin{aligned} M &= fR\cos(\psi+\varsigma) \overset{\text{linearized}}{\approx} f_0 R\sin 2\psi(\cos\psi-\varsigma\sin\psi) - f_{pilot}R(\cos\psi-\varsigma\sin\psi) = \\ &f_0 R\sin 2\psi(\cos\psi-\varsigma_0\sin\psi\cos(2\psi)) - f_{pilot}R(\cos\psi-\varsigma_0\sin\psi\cos(2\psi)) = \\ &f_0 R\left(\frac{1}{2}\sin 3\psi+\frac{1}{2}\sin\psi\right) - f_0\varsigma_0 R\left(\frac{1}{4}-\frac{1}{4}\cos 2\psi\right) - f_{pilot}R\cos\psi - f_{pilot}R\varsigma_0\left(\frac{1}{2}\sin 3\psi-\frac{1}{2}\sin\psi\right) \end{aligned} \tag{52}$$

This time the lead-lag moment M due to the lateral shaft motion contains a component in phase with the blade lead-lag velocity (40), and this component is introduced by the pilot force. Because the D'Alembert force alone cannot add energy to the system, it follows that energy can beaded to the system only via the pilot input force. Therefore, in this case energy is added from the shaft to the blade. The quantity of energy the system is fed via the rotor. For instability, this quantity has to be positive (energy is transmitted via the rotor as in order to sustain the oscillations). It means that when the pilot of reference [10] was stiffening his arm, he was transferring energy to the blade and had the term $f_{pilot}R\varsigma_0$ positive, driving unstable the high frequency advancing lead-lag mode. This conclusion shows that the physical approach considered in paper could determine the mechanism responsible for pilot-vehicle instability.

3. CONCLUSIONS

The main objective of this paper was to give a basic understanding of the mechanisms through which pilot cyclic inputs in lateral cyclic interacts with high-order rotor dynamics destabilizing the helicopter roll motion. In this sense, the paper gave a basic understanding how pilot excites the roll axis through unintentional stiffening his arm when flying more challenging tasks. Using a Newtonian approach for representing the forces in the system, it was demonstrated that both the lightly damped regressing lag mode and the advancing lag

mode may participate to the instability. Usually, the literature of specialty relates only to the regressing lag mode as this is close to the pilot's biodynamics mode. However, the paper demonstrated that the advancing lag mode can be critical for this instability when the pilot stiffens his arm. Future work will 1) consider numerical examples for pilot biodynamics gain and damping to determine more precisely his effect in the system and 2) implement the flapping dynamics in the system in order to determine how a stronger flap-lag coupling can transmit energy to the airframe roll motion.

REFERENCES

[1] R. E. Donham, S. V. Cardinale, I. B. Sachs, Ground and Air Resonance Characteristics of a Soft In-Plane Rigid-Rotor System, *J. of the American Helicopter Society*, **14**(4), pp. 33-41, Oct. 1969.

[2] Z. Xiao-gu, Physical Understanding of Helicopter Air and Ground Resonance, *J. of the American Helicopter Society*, **31**(4), pp. 4-11), Oct. 1986.

[3] R. A. Ormiston, Rotor-Fuselage Dynamics of Helicopter Air and Ground Resonance, *J. of the American Helicopter Society*, **36**(2), pp. 3-20, April 1991.

[4] R. P. Coleman and A. M. Feingold, *Theory of Self-Excited Mechanical Oscillation of Helicopter Rotors with Hinged Blades*, NACA TR-1351,1956.

[5] L. Robin, W. Jens, M. Hamers, *Increasing Handling Qualities and Flight Control Performance using an Air Resonance Controller*, 64thAnnual Forum of the American Helicopter Society, Montreal, Canada, April 29-May 1, 2008.

[6] B. R. Walden, *A Retrospective Survey of Pilot-Structural Coupling Instabilities in Naval Rotorcraft*, 63rd Annual Forum of the American Helicopter Society, Virginia Beach, VA, May 1-3, 2007.

[7] M. D. Pavel, et. al., Rotorcraft Pilot Couplings - Past, Present and Future Challenges. *Progress in Aerospace Sciences*, **62**, pp. 1-51. DOI:10.1016/j.paerosci.2013.04.003, 2013.

[8] M. D. Pavel, et. al., Practises to identify and prevent adverse aircraft-and-rotorcraft-pilot couplings: A design perspective, *Progress in Aerospace Sciences*, **76**, pp. 55-89. DOI:10.1016/j.paerosci.2015.05.002, 2015.

[9] M. D. Pavel, et. al., Practices to identify and preclude adverse Aircraft-and-Rotorcraft-Pilot Couplings – A ground simulator perspective, *Progress in Aerospace Sciences*, **77**, pp. 54-87. DOI:10.1016/j.paerosci.2015.06.007, 2015.

[10] G. Tod, M. D. Pavel, et. al., Understanding Pilot Biodynamical Feedthrough Coupling in Helicopter Adverse Roll Axis Instability via Lateral Cyclic Feedback Control, *Aerospace Science and Technology*, **59**, pp 18-31. DOI: 10.1016/j.ast.2016.10.003, 2016.

[11] V. Muscarello, G. Tod, et. al., *Adverse Aeroelastic Roll/Lateral Rotorcraft-Pilot Couplings Analysis*, 72nd Annual Forum of the American Helicopter Society, West Palm Beach, Florida, USA, May 17-19, 2016.

[12] M. D. Pavel, G. D. Padfield, *Understanding The Peculiarities of Rotorcraft - Pilot – Couplings*, 64th Annual Forum of the American Helicopter Society, Montreal, Canada, 2008.

[13] M. D. Pavel, *Modeling Lead-Lag Dynamics for Rotorcraft-Pilot-Couplings Investigation*, 66th Annual Forum of the American Helicopter Society, Phoenix Arizona, May 11-13, 2010.

[14] Z. Chikhaoui, M. D. Pavel, et. al., *Towards an Energetic Modeling of Rotorcraft Using Bond-Graphs*, 69th American Helicopter Society Annual Forum, 2013, Phoenix, Arizona.

[15] G. Quaranta, P. Masarati, J. Serafini, M. Gennaretti, Aeroelastic Rotorcraft-Pilot Couplings: Problems and Methods, *Aerotecnica Missili & Spazio The Journal of Aerospace Science, Technology and Systems*, **95**(3), pp. 176-187, 2016